Polarforschung 87 (1), 15 – 22, 2017

A Stratigraphical-Sedimentological Study of the Last Interglacial Period in the Central Nordic Seas on the Basis of XRF Core Scanning

by Henriette Kolling[1] and Henning A. Bauch[1,2]

Abstract: The recognition of specific geological time intervals is one of the major issues when establishing the stratigraphies of marine sediment cores. The automatic XRF core scanning method provides a fast and non-destructive method to precisely identify a given time interval and its changeable sedimentation histories. To test the applicability of XRF core scanning to recognize such periods, we studied in detail sedimentation processes across the last interglacial climate cycle (MIS 5e) on unsampled sediment core section from the central Nordic Seas – an area of high interest for paleoceanographic reconstructions. To further ground truth the XRF scanning results the core was sampled and the contents of iceberg-rafted debris (IRD) and shards of tephra were quantified. On that basis we identified Ti/Ca ratios as a potential indicator for IRD depositional peaks, and Ca as indicator of high biogenic carbonate production. Two well-known tephras from MIS 5e, Midt-RHY and 5e-low/Bas-IV, could be identified based on specific elemental content, such as Si, Ti, Zr, and Rb. By cross-core correlations using Ca-content and IRD-counts, the iceberg-free interval with enhanced deposition of biogenic carbonate lasted for about 9 ky, with a return of significant iceberg presence around 115 ka, notifying the onset of the last glacial inception. According to the age model applied we could further define the age of the 5e-Midt-RHY tephra at ~121.5 ka and of the 5e-low/Bas-IV at ~125.5 ka.

Zusammenfassung: Für die stratigraphische Einordnung von Sedimentkernen ist die Identifikation von bestimmten geologischen Zeitintervallen von großem Interesse. Der Röntgenfluoreszenz (XRF) Kernscanner bietet eine schnelle, zerstörungsfreie Methode, um ein bestimmtes Zeitintervall und dessen Sedimentationsgeschichte präzise zu identifizieren. Am Beispiel des letzten Interglazial (MIS 5e) wurde die Anwendbarkeit des XRF-Kernscanners für die Identifikation spezifischer geologischer Zeitabschnitte an einem unbeprobten Sedimentkernabschnitt aus dem europäischen Nordmeer getestet. Die XRF-Messungen wurden durch Beprobung des Kerns und anschließende Untersuchung auf enthaltenes eistransportiertes Material (IRD) und vulkanische Aschepartikel validiert. Auf Basis dieser Ergebnisse konnte das Ti/Ca-Verhältnis als möglicher Anzeiger für IRD-Gehalt und Kalziumkonzentrationen als Indikator für hohe biogene Karbonatgehalte im Sediment erkannt werden. Die Lage zweier bekannter Aschelagen aus dem MIS 5e, (Midt-RHY und 5e-low/Bas-IV) konnten mittels spezifischer Konzentrationen von Si, Ti, Zr und Rb genauer dargestellt werden. Durch Kern-Korrelation anhand von Ca- und IRD-Gehalten wurde dem MIS 5e-Intervall, das durch geringe IRD-Gehalte und erhöhte Ablagerung von biogenem Karbonat charakterisiert ist, eine Dauer von etwa 9 ky zugeordnet. Der Beginn des letzten Glazials wurde mit dem vermehrten IRD-Vorkommen auf 115 ka datiert. Basierend auf dem angewendeten Altersmodell konnte der Asche 5e-Midt-RHY ein Alter von ~121,5 ka und der Asche 5e-low/Bas-IV ein Alter von ~125,5 ka zugeordnet werden.

Keywords: Nordic Seas, MIS 5e, XRF core scanning, tephra, IRD

doi:10.2312/polarforschung.87.1.15

[1] Alfred Wegener Institute Helmholtz Centre for Polar and Marine Research, Bremerhaven, Am Alten Hafen 26, D-27568 Bremerhaven, Germany, <Henriette.Kolling@awi.de>

[2] GEOMAR Helmholtz Centre for Ocean Research, Wischhofstraße 1-3, D-24148 Kiel, Germany.

This paper was presented as an oral report at the conference „Das Klima der Arktis – Ein Frühwarnsystem für die globale Erwärmung“ at the Akademie der Wissenschaften und der Literatur zu Mainz, 02-03 November 2016.

Manuscript received 04 August 2017; accepted in revised form 05 September 2017.

INTRODUCTION

The Nordic Seas are regarded as one of the most sensitive areas for climate change in the world's oceans (Schäfer et al. 2001) and are of great paleoclimatic interest due to the deep water formation that takes place in this area (Hopkins 991). Thus, a high number of sediment cores from this region have been collected and analysed in several recent, higher-resolution paleoceanographic studies (Solignac et al. 2004, Helmke et al. 2005, Bendle & Rosell-Melé 2007, Van Nieuwenhove et al. 2008, Fauria et al. 2010, Risebrobakken et al. 2011, Bauch et al. 2012, Dylmer et al. 2013, Telesiński et al. 2014, Latarius & Quadfasel 2016).

The geochemistry of marine sediment cores may provide essential information for both, core-to-core correlation as well as palaeoceanographic and climatic reconstructions. In this respect, the non-destructive approach of X-ray fluorescence (XRF) sediment core scanning allows to detect specific geochemical features in sediment cores, as it can measure the elemental composition down to a very high spatial resolution directly from the sediment surface. This method has proven useful in many studies over the past decade (Tjallingii 2006, Ziegler et al. 2008, Hodell et al. 2010, Channell et al. 2012, Channell & Hodell 2013, Ohlendorf et al. 2015). In the Nordic Seas, only few studies have applied this method for stratigraphic purposes (Helmke et al. 2005, Brendryen et al. 2010) or for the identification of discrete events, e.g., volcanic eruptions (Kylander et al. 2012).

Here, we present an approach to classify the sediment composition of the last interglacial (Eemian or MIS 5e) in the central Nordic Seas (Fig. 1). Since past warm phases are of interest in respect to the expected global warming in general, MIS 5e has long been referred to as suitable analogue to the recent and future global warming (Kellogg 1980). Hence, it is of further interest to develop methods and proxies to better define the climate character of this period in any type of depositional setting. In the Nordic Seas, MIS 5e reveals a very straightforward climate development: It is preceded by a glacial maximum with high input of ice-rafted-debris (IRD), MIS 6 (or Saalian), followed by MIS 5e of warm, interglacial conditions with no IRD but high biogenic carbonate production (Bauch et al. 2012). The terminal phase of MIS 5e is characterized by a return of IRD due to global cooling and the inception of the youngest glaciation, the Weichselian (Sejrup et al. 1995, Bauch 1996, Bauch & Helmke 1999, Didié et al. 2002, Rasmussen et al. 2003, Hibbert et al. 2010). Accompanied is the last interglacial cycle by a conspicuous drop and rise in marine $\partial^{18}O$, which commonly reflects the combined effect of changes in global ice volume and local ocean temperature.

In this study we aim to investigate the applicability of XRF core scanning to identify certain geological time periods based on specific geochemical characteristics and volcanic tephra layers. We attempt to identify MIS 5e in an unsampled sediment core based on its geochemical composition and the correlation to a well-dated neighbouring core. In a second step the semi-quantitative XRF results are compared with and evaluated against quantified results of IRD and ash grains.

MATERIAL & METHODS

Core Material

In this study sediment core MD992276 from the centre of the Nordic Seas was analysed (69°21.94' N, 6°32.36' W, 2710 m, Fig. 1). This core was taken at the lower slope of Jan Mayen Ridge with a Calypso piston corer in 1999 during the research campaign IMAGES V (GHERADI et al. 1999). For stratigraphic correlation, core MD992276 (MD76) is directly compared with relevant data from neighbouring cores PS1243 (69°22' N, 6°32' W, 2710 m, AUGSTEIN et al. 1984) and MD992277 (69°15.01' N, 6°19.75' W, 2800 m, GHERADI et al. 1999).

Sediment Characteristics

Contents of biogenic carbonate, which mainly represent the variable amount of foraminifers and coccoliths, and IRD are major constituents in sediment cores from the Nordic Seas and reflect the hemipelagic depositional environment of the region (WOLF & THIEDE 1991). Larger lithic grains, which eventually melt out from icebergs, are transported farther from the site of their entrainment by wind and surface currents (LISITZIN 2002). IRD in the Nordic Seas is therefore a very useful proxy for iceberg drift related to glacial-interglacial changes as these are linked to the climate-driven waxing and waning of glaciers on the surrounding continents (FRONVAL & JANSEN 1997, HELMKE et al. 2005).

Another characteristic feature in sediment cores from the Nordic Seas are tephra layers. Tephras are unconsolidated ash particles that originate from volcanic eruptions (THORARINSSON 1944). Due to their specific geochemical composition it is possible to trace back tephras in the Nordic Seas to the originating volcanic system and a single eruptive event (LACASSE & GARBE-SCHÖNBERG 2001, WALLRABE-ADAMS & LACKSCHEWITZ 2003, BRENDRYEN et al. 2010). Thus specific tephra layers not only provide a good tool to improve core-to-core correlations they also allow to more precisely put different paleoenvironmental records onto a common time scale (RASMUSSEN et al. 2003). An example for such a relevant tephra is a ryholitic layer that was deposited in areas of the southern Nordic Seas during the mid-Eemian and which has been applied as a stratigraphic marker for this time interval (FRONVAL & JANSEN 1997, FRONVAL et al. 1998, SJØHOLM et al. 1991). This specific tephra is often referred to as 5e-Midt-RHY (Rhy-5e) and is characterized by high concentrations in silicon (Si), aluminium (Al), sodium (Na) and potassium (K) (LACASSE 2001, WASTEGÅRD & RASMUSSEN 2001). Further, a basaltic tephra termed 5e-low/Bas-IV (Bas-IV) is characterized by high Ca, Al, and Fe concentrations and has been found near the end of the Saalian deglaciation (Termination 2) in several sediment records from the Nordic Seas (e.g., SJØHOLM et al. 1991, LACASSE et al. 1996, WASTEGÅRD & RASMUSSEN 2001).

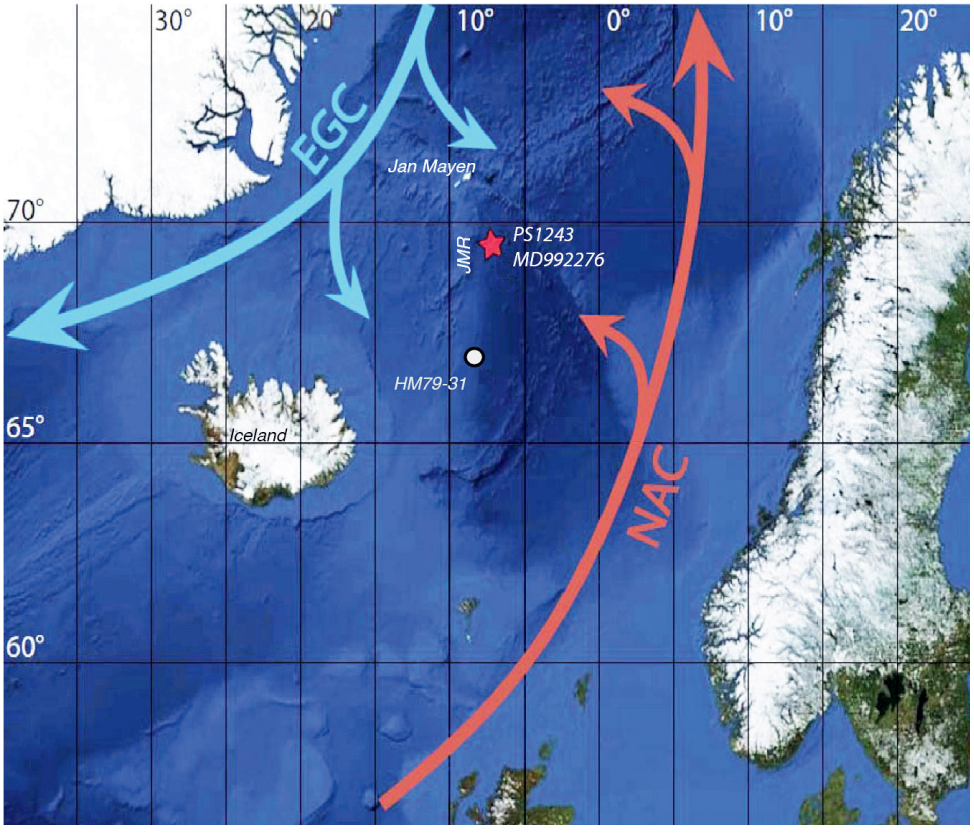

Fig. 1: Surface circulation scheme in the Nordic Seas between Greenland and Scandinavia showing cold (blue) East Greenland Current (EGC) and warm (red) Norwegian Atlantic Current (NAC). Red star denotes location of site MD76/77 and PS1243 at the lower eastern slope of Jan Mayen Ridge (JMR). Also indicated is the location of core HM79-31 (FRONVAL et al. 1998).

Abb. 1: Schematische Darstellung der Oberflächenzirkulation im europäischen Nordmeer zwischen Grönland und Skandinavien. Blau: Ostgrönland Strom (EGC). Rot: Norwegen Atlantik Strom (NAC). Roter Stern: Lokation der Kerne MD76/77 und PS1243 am östlichen Hang des Jan Mayen Rückens (JMR). Gelber Punkt: Lokation des Kerns HM79-31 (FRONVAL et al. 1998).

XRF Scanning

For our study we employed the computer-controlled *Aavatech* XRF core scanner, with an Oxford rhodium (Rh) x-ray source. Settings for XRF scanning are shown in Table 1.

To avoid an overprint of the background signal and measurement differences only element-element ratios or ratios of a single element against the mean of all element ratios (expressed as "element/sum") will be used.

IRD & Tephra

To investigate the amounts of IRD and tephra content (Fig. 2), the core was sampled by cutting 1 cm thick slices from the core. Samples were then freeze-dried and later washed over a 63 μm mesh. After drying, the residue material was sieved over a 150 μm mesh to create two size fractions of each sample. IRD grains were counted in the larger size fraction. The fraction <150 μm was not considered as this grain size may not be exclusively related to ice rafting processes but also to other processes, e.g., ocean currents, sea-ice transport. For further quantifications samples were split down with a micro splitter to a size that could be distributed equally on a tray. Counted grains are expressed as IRD grains per gram of dry bulk sediment.

Rhyolitic tephra shards were counted in the same way as IRD, but in the fraction <150 µm. The content of tephra shards of the whole sample was calculated and expressed as shards per gram of dry bulk sediment. Because of the likelihood of a mixed origin between basaltic material derived from volcanic islands (Iceland, Jan Mayen) via ice transport and the low amounts of BAS-grain material, the stratigraphic position of the BAS is exclusively determined by geochemical XRF-scanning and comparison with other proxy records.

1. Run	2. Run
Tube Voltage: 10 kV	Tube Voltage: 30 kV
Tube Current: 250 μA	Tube Current: 1000 μA
Count Time: 15 s	Count Time: 20 s
Slit Size (down core): 2 mm	Slit Size (down core): 2 mm
Slit size (cross core): 12 mm	Slit size (cross core): 12 mm
Filter: No Filter	Filter: Pd-thick
Step Size: 5 mm	Step Size: 2 mm

Tab. 1: XRF-scanner settings for the two runs applied:

Tab. 1: Verwendete Einstellungen für zwei Messläufe mit dem Röntgenfluoreszenz (XRF) Kernscanner.

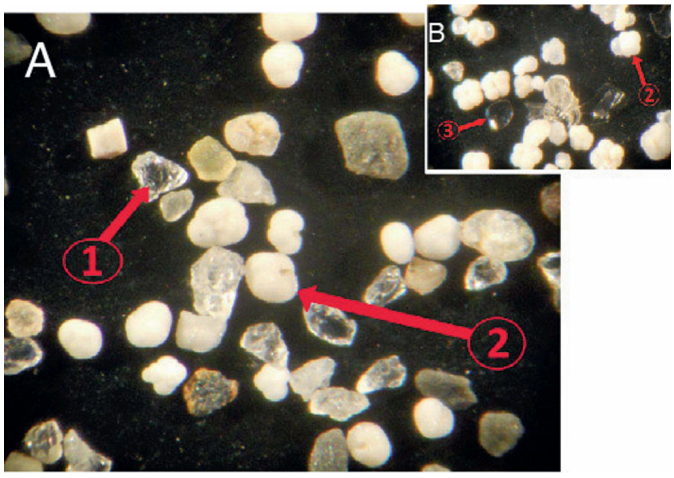

Fig. 2: Washed sample residues from core MD992276 (>150 μm) showing typical glacial (cold) constituents in (A) and warm, last interglacial components in (B). 1: Ice rafted detritus (IRD); 2: planktic foraminifer; 3: volcanic glass shards of the Rhy-5e tephra.

Abb. 2: Die gewaschenen Proben (>150 μm) des Sedimentkerns MD992276 zeigen typische Komponenten für (A) glaziale (kalte) und (B) interglaziale (warme) Phasen. 1: Eisbergtransportiertes Material (IRD); 2: planktische Foraminiferen; 3: vulkanische Glasscherben der Rhy-5e-Asche.

RESULTS

Stratigraphy

The interval of the last interglacial period, marine isotope stage MIS 5e, in core MD-76 is clearly determined by comparisons with previously gained data from the neighbouring cores MD77 and PS1243 (Fig. 3). Both Ca-count records measured on cores MD-76/77 compare extremely well with actually measured $CaCO_3$ (%) values on the bulk sediment of core PS1243. The good match among all three cores further reveals that the analysed section between 520 and 300 cm in MD-76 relates to the late glaciation of MIS 6 and the substage MIS 5a.

Records of IRD and tephra

In most samples ice-rafted material is present in the fraction >150 μm. Across the peak of MIS 5e, between 433 and 387 cm, the IRD records show no or a very low content in lithic grains. In contrast several peaks with exceptionally high IRD concentrations are noticeable during MIS 6 but are also found above MIS 5e, i.e. ~512 cm (~5000 grains/g) and ~322 cm (~4500 grains/g; Fig 4).

The core section between 415 and 400 cm is marked by the occurrence of a distinct tephra horizon (Fig. 4). The highest concentrations of shards exist at 409 cm with ~1700 shards/g dry sediment (56 shards/cm^3). The tephra consists of rhyolitic, glassy, cuspate shards (Fig. 2) with a dominance in the fraction of 63-150 μm. Previous chemical investigations on nearby cores have shown this to be the Rhy-5e tephra layer (Fronval et al. 1998, Wallrabe-Adams & Lackschewitz 2003).

Geochemical composition

Throughout the core Ca counts show enhanced variability (Fig. 4), but highest values are to be found between 425 and 385 cm. These high values are significantly decreased during the deposition of the tephra horizon. Above MIS 5e, low Ca content is generally dominant between 380 and 320 cm, with a return to increased Ca values found during MIS 5a.

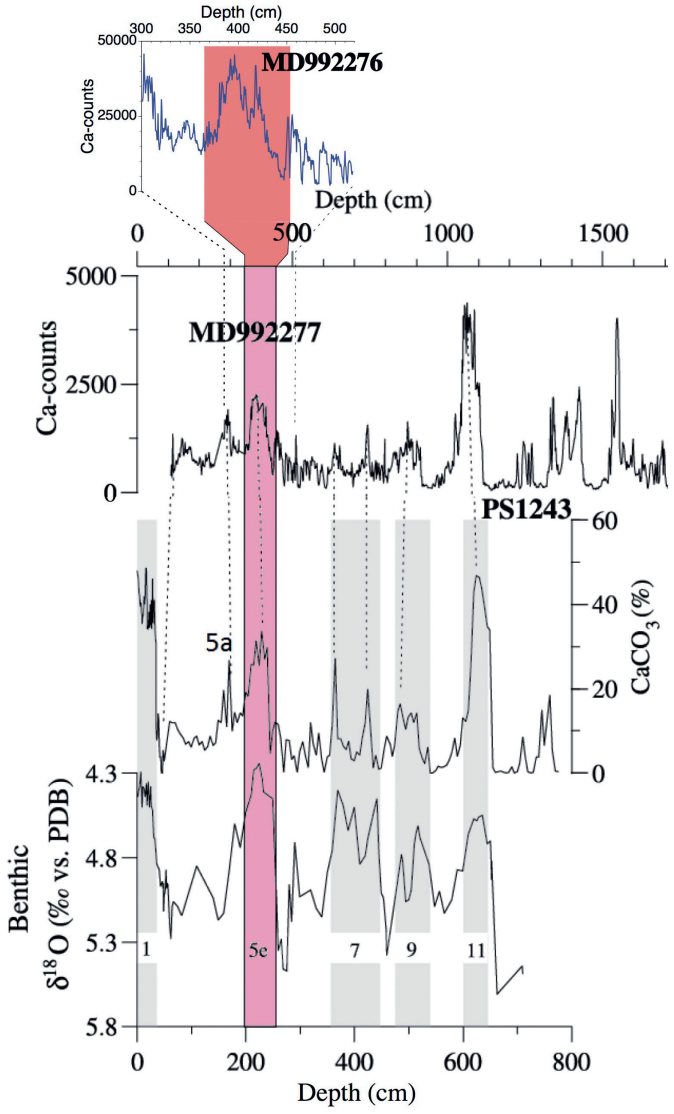

Fig. 3: Core-to-core correlation scheme showing the investigated interval of core MD992276 *versus* existing records from cores PS1243 and MD992277 (HELMKE et al. 2005).

Abb. 3: Schematische Korrelation des untersuchten Intervalls von Sedimentkern MD992276 mit publizierten Daten der Sedimentkerne PS1243 und MD992277 (HELMKE et al. 2005).

The Ti/Ca ratio, which is inversely related to biogenic carbonate, shows a similar high variability with a series of prominent peaks in the lowest core section addressed to late MIS 6 and Termination 2. Such a good visual correlation with the terrigenous IRD material is more muted throughout the rest of the record where the Ti/Ca ratio stays comparatively low with only minor peaks (Fig 4).

As has been shown before (BRENDRYEN et al. 2010) both Ti/K and magnetic susceptibility (MS) correspond usually well to one another by showing low values during times of high Ca contents. However, a strong correlation of the two with IRD matches only occasionally. For instance, the highest peak in Ti/K and MS is recognized around 360 cm core depth, but they show no obvious relation to any enhanced IRD deposition at this core depth. That would point to the type of sediment, e.g., titanium-rich basaltic material, as the main factor determining the MS signal.

The 2-mm-step, high-resolution second run of XRF-scan supports the above-mentioned notion on the type of sediment particles. Although to a strongly varying degree, the two element ratios Rb/sum and Zr/sum do show a positive response during late Termination 2 – the potential stratigraphic position of the Bas-IV – and across the Rhy-5e tephra layer, between 446-432 cm and 414-405 cm core depth (Fig. 4e-d). However, while Rb/sum as well as Si/Sr ratios are both markedly enhanced together at the base of the Rhy-5e layer, Zr/sum and Rb/sum are less conclusive during the later phase of Termination 2. And yet, there is a prominent, 1 cm thick spike in Zr/sum at 433.5 cm, which falls broadly together with a maximum in MS and Ti/sum. We consider this spike to be representative of the Bas-IV tephra layer, also because we note just below both tephras a significant increase in Mn/sum (Fig. 4c) likely as a result of reduced conditions at the sea floor.

DISCUSSION

Detection of IRD by XRF core scanning

As an important sedimentary feature indicative for changes in iceberg flux and ice sheet growth (BAUMANN et al. 1995. FRONVAL & JANSEN 1997) IRD is of high interest and detection and geochemical analysis with XRF scanning may provide a fast tool to receive detailed downcore information. The close correlation of IRD and Ti/Ca peaks (Fig. 4) we interpret as a signal of relative reduction of biogenic, marine-produced $CaCO_3$, due to a diluting effect of increased terrigenous IRD grains rich in Ti relative to the background sediment. That Ti/Ca ratios do show at times a different intensity relative to the IRD peaks may be partly caused by different iceberg pro-venances. A clearer identification of the source regions may be possible with the ratios of Ti/Sr, and Si/Sr (CHANNELL & HODELL 2013), which are not available for our record due to our chosen instrument settings. To test the applicability of XRF scanning to measure geochemical composition and source region of IRD layers further ground-truthing, e.g. with XRD measurements would be necessary. When detecting IRD by XRF core scanning possible effects of changes in grain size, surface roughness and pore water content on the results need to be taken into account. Because these factors are minimised somewhat by the use of elemental ratios, we assume our results reliable and consider Ti/Ca ratios a solid indicator for IRD layers in this part of the Nordic Seas.

Detection of tephra layers

Specific tephra layers provide excellent geochronological markers in the Nordic Seas and when compared to other records may allow for a precise age correlation between them (RASMUSSEN et al. 2003). In regions affected by ice rafting like the Nordic Seas tephras may also be deposited by melting from sea ice and icebergs. To become an ideal stratigraphic time marker a rapid deposition to the sea floor is required. Therefore, ice-rafted (by sea-ice and/or icebergs) tephras should not be considered as such. The tephra layer in core MD76 was deposited during a time with no IRD deposition (Fig. 4). The lack of IRD may point towards a reduction in ice rafting in general and therefore may indicate tephra transport by atmo-

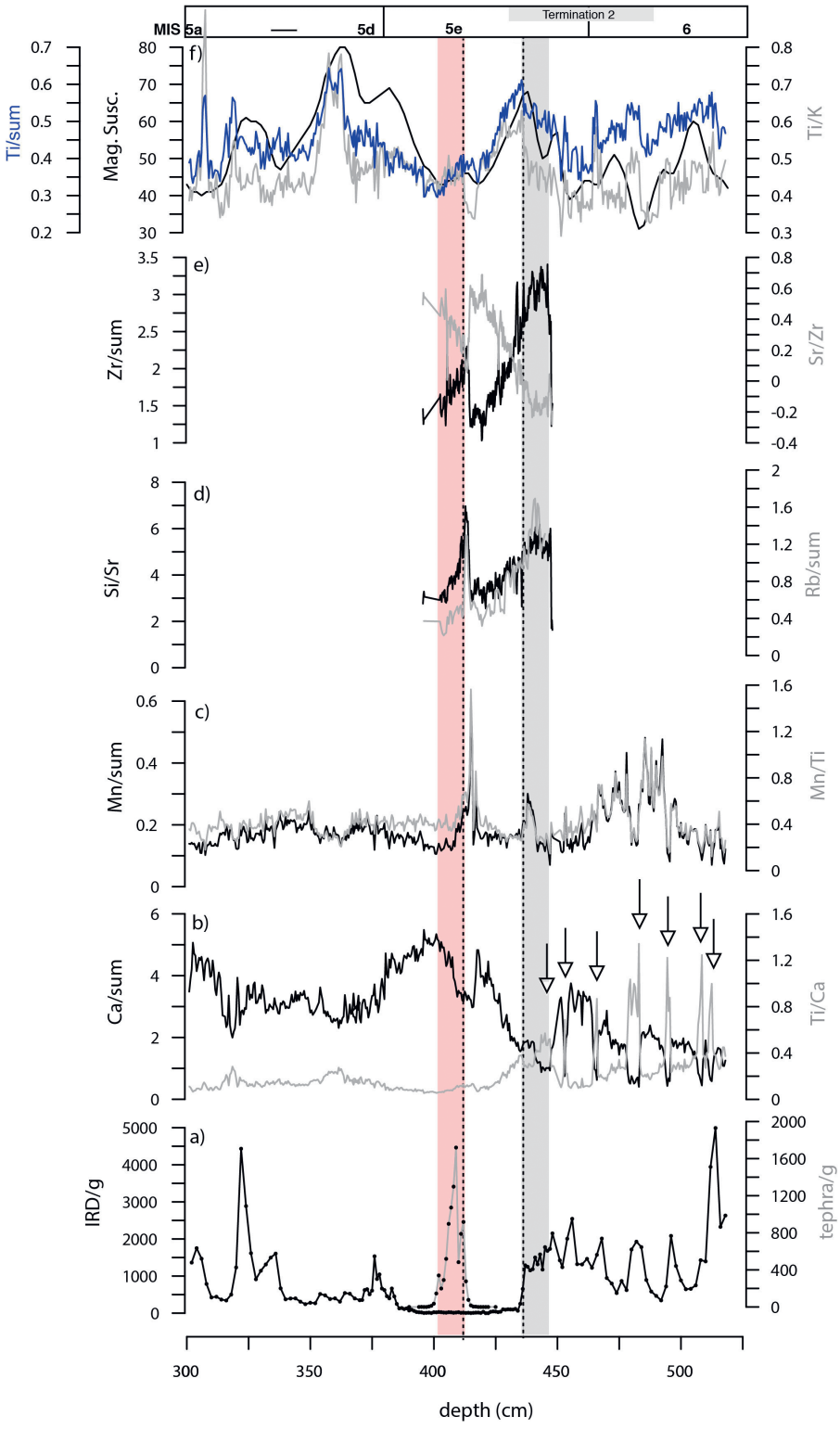

Fig. 4: XRF-scanning of core MD992276 for the interval spanning from MIS 6 into late MIS 5a (f) in comparison with quantified results of grains of IRD and tephra (a); data shown in (d) and (e) refer to the second run (see Tab. 1). Grey vertical bar denotes the potential interval of tephra Bas-IV deposition and the pink bar the distribution of Rhy-5e glass shards (4a). Stippled lines mark the actual stratigraphic position of the eruption event of the two tephras.

Abb. 4: Ergebnisse des Röntgenfluoreszenz (XRF) Kernscans des Sedimentkerns MD992276 für das Intervall zwischen MIS 6 und MIS 5a (f) und Gehalten von IRD und Asche (a). Die in (d) und (e) dargestellten Daten beziehen sich auf den zweiten XRF-Messdurchlauf (vgl. Tab. 1). Der graue senkrechte Balken bezeichnet die mögliche Lage der Asche Bas-IV im Sedimentkern. Der rosa Balken zeigt das Vorkommen von Glasscherben der Rhy-5e-Asche (a). Die gestrichelten Linien markieren die ermittelte stratigraphische Position des Eruptionsereignisses der beiden Aschen.

spheric and oceanic circulations. The shard size limitation of <150 mm may, however, suggest subaerial transfer as the main transporting agent. Thus, we consider a small time lag between eruption and deposition of the tephra layer in core MD76, and consider this Rhy-5e layer a sound geochronological marker.

Geochemical analyses on discrete grains of tephra (e.g., by microprobe) may provide information on a certain volcanic system or even on specific eruptions of the same event. For both Rhy-5e as well as Bas-IV this has been shown to be the case, and further that both tephras do relate to the Icelandic volcanic complex (e.g., Brendryen et al. 2010). According to Kylander et al. (2012) the detection of tephra layers with XRF scanning would require enhanced tephra concentrations (>850 shards/cm^3). In spite of much lower concentrations estimated for core MD76 (~50 shards/cm^3) we do see clear evidence in our XRF geochemical records for a detection of the tephra layers in the sediment.

It is intriguing to note from the XRF records the occurrence of a prominent Mn/sum peak just below the two tephras (Fig. 4). Although a number of reasons may be possible for Mn enriched layers in the polar oceans (MÄRZ et al. 2011), Mn has been reported as an indicator for tephras and volcanic activity (KYLANDER et al. 2012). The Mn/sum concentrations in our record appear clearly associated with the tephra themselves. The tephra grains, their chemistry and rapid deposition probably affected the oxygenation of the sediment and pore water below leading to a redox milieu that favoured a concentration of Mn.

High concentrations of Si/sum and lowered Ca/sum concentrations in the sediment (Fig. 4) indicate that our Rhy-5e is the one previously described also by others (SJØHOLM et al. 1991, FRONVAL & JANSEN 1997, FRONVAL et al. 1998, BRENDRYEN et al. 2010). Its geochemistry is characterized by high Si, Al, Na and K as well as low Ca concentrations (LACASSE 2001, WASTEGÅRD & RASMUSSEN 2001). The distinct peak in the Si (Si/Sr ratio) at the base of Rhy-5e (Fig. 4d) reveals a relative increase of inorganic silicon, which, due to the absence of IRD and especially quartz grains during this period, is therefore related to the glassy shards of the rhyolite tephra. The gradually increasing Sr/Zr ratios and Ca/sum across this core section may indicate a diluting effect of the tephra shards on the biogenic carbonate. Thus the reduction of Ca/sum should not be seen as a reduction in calcium bioproductivity, i.e., in foraminifers, but as a time of very rapid deposition of the tephra material.

The elevated element Rb/sum correlates with the base of the rhyolitic tephra layer (Fig. 4d). Whether this element concentration was associated with the distinct geochemistry of the tephra/originating volcanic system or is caused by geochemical processes in the sediment cannot be determined from the data available. High Rb/sum contents have not been reported explicitly for Icelandic systems but has been associated with tholeiitic and low-potassium alkali lavas, e.g., in Hawaii (LESSING et al. 1963). In contrast, the high K that we note just below and during the base of the Rhy-5e layer (Fig. 4f) corroborates geochemical analyses which show potassium content of Rhy-5e to be about 10-fold higher than in the low-potassium Bas-IV tephra (FRONVAL et al. 1998). Taking all the elemental features together it seems evident that the base of the Rhy-5e layer is the actual eruptive event, and that the presence of the shards further up the core (Fig. 4a) are primarily the post-sedimentary result of bioturbational activity.

Although identified in several sediment cores from the Nordic Seas (SJØHOLM et al. 1991, LACASSE et al. 1996, FRONVAL et al. 1998, WASTEGÅRD & RASMUSSEN 2001), the Bas-IV was not so evident in core MD76. Considering the treatment of the sediment (i.e. storage, washing, sieving), the basaltic tephra nodules may have been disintegrated into smaller grains than the size fraction considered by us. In the XRF record, however, we see chemical evidence for this existence of a tephra layer in peaks of Zr/sum and Ti/sum, as well as Mn/sum, just below. The major peak in Ti/sum (and Zr/sum) in the Bas-5e versus the low values found in Rhy-5e is in accordance with a 3 to 4 times higher Ti-content measured analytically in Bas-IV grains (FRONVAL et al. 1998, WASTEGÅRD & RASMUSSEN 2001).

Stratigraphic implications

Sediment cores from the southern Nordic Seas show that glacial-interglacial quantitative records of foraminifers shells (number/g) match very closely the trends in bulk $CaCO_3$ contents (BAUCH et al. 2001). And, in similar fashion, we could show that also the Ca data derived from XRF-scanning corresponds to variations in the bulk $CaCO_3$ (Fig. 3). We now employ that type of information to make some further assumptions on core-to-core correlations as well as age model differences.

In nearby core PS1243, Rhy-5e has also been clearly documented (BAUCH et al. 2012), and the same is true for core HM79-31 (FRONVAL et al. 1998), which is located to the south of site MD76/PS1243 (Fig. 1). Across the last interglacial cycle PS1243 shows the typical reduction of IRD during the peak of MIS 5e with the rhyolitic tephra in its centre and generally low planktic foraminiferal $\partial^{18}O$ (Fig. 5) – this phase lasted in total not longer than 9 ky. As in MD76, the Bas-IV tephra

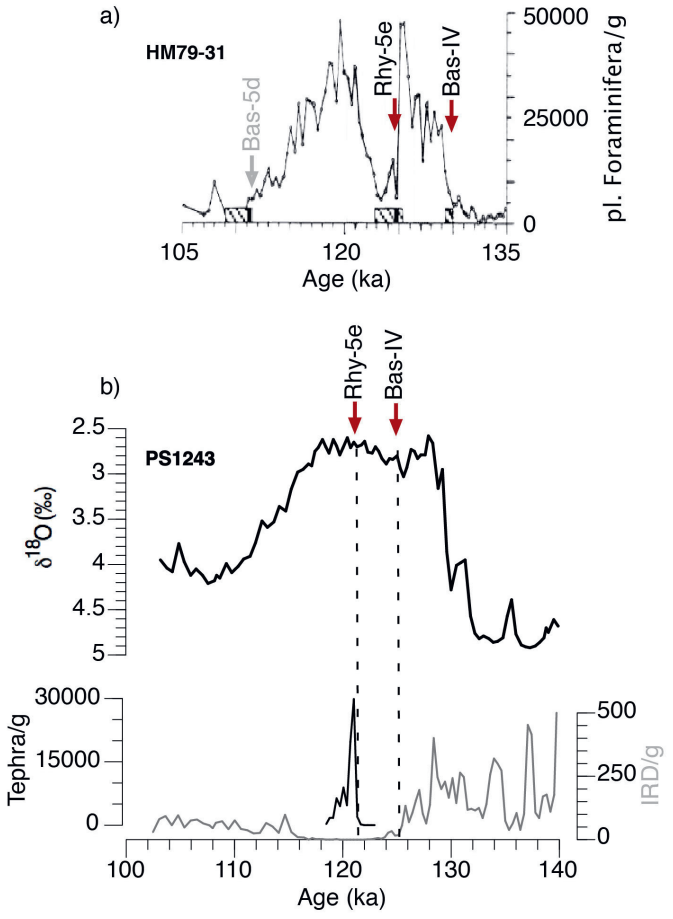

Fig. 5: Age assignments of the two tephras during MIS 5e from two sites of the central Nordic Seas; each core being on its independent age model. (a): Core HM79-31 showing (peak of tephra grains denoted as vertical black bars (FRONVAL et al. 1998). Also shown is the position of the youngest tephra BAS-5d. b) Stratigraphic records of core PS1243 with tephra positions across MIS 5e.

Abb. 5: Alterszuordnung der beiden Aschelagen aus dem MIS 5e an zwei Lokationen im europäischen Nordmeer, wobei jedem Kern ein unabhängiges Altersmodell zugeordnet ist. (a): Kern HM79-31 (die Aschelagen, wie auch die Lage der jüngsten Asche BAS-5d, sind als schwarze Balken angedeutet (FRONVAL et al. 1998). (b) Stratigraphische Darstellung von Kern PS1243 mit Aschelagen und der Positionen des MIS 5e.

is positioned at the end of main IRD deposition (Termination 2), which corresponds well to all other studies in which this ash has been identified (e.g. FRONVAL et al. 1998, RASMUSSEN et al. 2003). Comparing the Ca-record in MD76 (Fig. 4b) with the foraminiferal data of core HM79-31 con-firms our correct stratigraphic positioning of the two ash layers.

A major difference between HM79-31 and PS1243 arise from the age assignments of the two ash layers. The age model of PS1243 shown in Figure 5 is based on correlations with the latest AICC2012 gas age model (ZHURAVLEVA et al. 2017). Accordingly, the age of Rhy-5e is ~121.5 ka and that of Bas-IV ~125.5 ka. These ages are significantly younger than those originally proposed by FRONVAL et al. (1998), but more similar to those given by RASMUSSEN et al. (2003).

Although not a focus of this study here, HM79-31 also shows a younger ash at ~111 ka (Fig. 5a) which is primarily comprised of basaltic material (FRONVAL et al. 1998). Because Ti (and Ti/K) agrees so well with MS (BRENDRYEN et al. 2010), we can clearly recognize this so-called 5d-ash in the corresponding XRF-data at around 360 cm core depth (Fig. 4a).

CONCLUSIONS

XRF core scanning was applied to investigate the elemental composition on a sediment core from the Nordic Seas spanning the time interval from MIS 6, across the MIS 5e interglacial, and into late MIS 5. The method proved to be a very valuable tool to identify not only contrasting time intervals such glaciations and interglacial periods, it can also be utilized successfully to identify discrete events such as tephra layers. Comparing records of IRD with XRF data we could determine the Ti/Ca ratio as a geochemical indicator for IRD in the Nordic Seas. The identification of tephra layers via XRF was possible in spite of low shard concentrations. Although the detailed geochemical composition of the tephra remains somewhat unclear, probably because of overprint by the sediment matrix, certain characteristic elements can still be used with success to distinguish the mid-5e rhyolitic tephra layer from the basaltic ash in the early MIS 5e. Moreover, with the help of cross-core-correlations we could determine the ages of the two tephra layers. Accordingly, the deposition of the rhyolitic tephra 5e-Midt-RHY occurred at ~121.5 ka and the basaltic tephra 5e-low/Bas-IV at ~125.5 ka.

ACKNOWLEDGMENTS

The authors would like to thank Dieter Garbe-Schönberg, Institute for Geoscience at Kiel University, for support with XRF measurements and the interpretation of XRF data. We are grateful to anonymous review comments, which helped to improve the manuscript.

References

Augstein, E., Hempel, G., Schwarz, J.N., Thiede, J. & Weigel, W. (1984): Die Expedition ARKTIS II des FS „POLARSTERN“ 1984 mit den Beiträgen des FS „Valdivia“ und des Forschungsflugzeuges „Falcon 20“ zum Marginal Ice Zone Experiment (MIZEX).- Rep. Polar Research 20: 1-192.

Bauch, H.A. & Helmke, J.P. (1999): Glacial-interglacial records of the reflectance of sediments from the Norwegian – Greenland – Iceland Sea (Nordic seas).- Int. J. Earth Sci. 88: 325-336.

Bauch, H.A., Struck, U. & Thiede, J. (2001): Planktic and Benthic Foraminifera as Indicators for Past Ocean Changes in Surface and Deep Waters of the Nordic Seas.- In: P. Schäfer, W. Ritzrau, M. Schlüter & J. Thiede (eds), The Northern North Atlantic: A Changing Environment, Springer, New York, 411-421.

Bauch, H.A., Kandiano, E.S. & Helmke, J.P. (2012): Contrasting ocean changes between the subpolar and polar North Atlantic during the past 135 ka.- Geophys. Res. Lett. 39: 1–7, doi: 10.1029/2012GL051800

Bauch, H.A. (1996): Monitoring Termination II at high latitude: anomalies in the planktic foraminiferal record.- Mar. Geol. 131: 89-102, doi: 10.1016/0025-3227(95)00147-6

Baumann, K.H., Lackschewitz, K.S., Mangerud, J., Spielhagen, R.F., Wolfwelling, T.C.W., Henrich, R. & Kassens, H. (1995): Reflection of Scandinavian ice-sheet fluctuations in Norwegian sea sediments during the past 150,000 years.- Quat. Res. 2: 185-197

Bendle, A.P. & Rosell-Melé, A. (2007): High-resolution alkenone sea surface temperature variability on the North Icelandic Shelf: implications for Nordic Seas palaeoclimatic development during the Holocene.- The Holocene 17: 9-24, doi: DOI: 10.1177/0959683607073269

Brendryen, J., Haflidason, H. & Sejrup, H.P. (2010): Norwegian Sea tephrostratigraphy of marine isotope stages 4 and 5: Prospects and problems for tephrochronology in the North Atlantic region.- Quat. Sci. Rev. 29: 847-864, doi: 10.1016/j.quascirev.2009.12.004

Channell, J.E.T. & Hodell, D.A. (2013): Magnetic signatures of Heinrich – like detrital layers in the Quaternary of the North Atlantic.- Earth Planet. Sci. Lett. 369/370: 260-270, doi: 10.1016/j.epsl.2013.03.034

Channell, J.E.T., Hodell, D.A., Romero, O., Hillaire-Marcel, C., de Vernal, A., Stoner, J.S., Mazaud, A. & Röhl, U. (2012): A 750-kyr detrital-layer stratigraphy for the North Atlantic (IODP Sites U1302-U1303, Orphan Knoll, Labrador Sea).- Earth Planet. Sci. Lett. 317/318: 218-230, doi: 10.1016/j.epsl.2011.11.029

Didié, C., Bauch, H.A. & Helmke, J.P. (2002): Late Quaternary deep-sea ostracodes in the polar and subpolar North Atlantic: Paleoecological and paleoenvironmental implications.- Palaeogeogr. Palaeoclimatol. Palaeoecol. 184: 195-212, doi: 10.1016/S0031-0182(02)00259-6

Dylmer, C.V., Giraudeau, J., Eynaud, F., Husum, K. & De Vernal, A. (2013): Northward advection of Atlantic water in the eastern Nordic Seas over the last 3000 yr.- Clim. Past 9: 1505-1518, doi: 10.5194/cp-9-1505-2013

Fauria, M.M., Grinsted, A., Helama, S., Moore, J., Timonen, M., Martma, T., Isaksson, E. & Eronen, M. (2010): Unprecedented low twentieth century winter sea ice extent in the Western Nordic Seas since A.D. 1200.- Clim. Dyn. 34: 781-795, doi: 10.1007/s00382-009-0610-z

Fronval, T. & Jansen, E. (1997): Eemian and Early Weichselian (140-60 ka) Paleoceanography and paleoclimate in the Nordic Seas with comparisons to Holocene conditions.- Paleoceanography 12: 443-462, doi: 10.1029/97PA00322

Fronval, T., Jansen, E., Haflidason, H. & Sejrup, H.P. (1998): Variability in surface and deep water conditions in the Nordic Seas during the last interglacial period.- Quat. Sci. Rev. 9-10: 963-985.

Gheradi, J-M., Labeyrie, L., Cortijo, E., Jansen, E. & Balut, Y. (1999): Campagne Interpole MD99-114/IMAGES V Atlantique Nord et Mers Actiques. Les Rapports de Campagne a la Mer a Bord Du Marion-Dufresne. Cruise Report.

Helmke, J.P., Bauch, H.A., Röhl, U. & Mazaud, A. (2005): Changes in sedimentation patterns of the Nordic seas region across the mid-Pleistocene.- Mar. Geol. 215: 107-122, doi: 10.1016/j.margeo.2004.12.006

Hibbert, F.D., Austin, W.E.N., Leng, M.J. & Gatliff, R.W. (2010): British ice sheet dynamics inferred from North Atlantic ice-rafted debris records spanning the last 175 000 years.- J. Quat. Sci. 25: 461-482, doi: 10.1002/jqs.1331

Hodell, D.A., Evans, H.F., Channell, J.E.T. & Curtis, J.H. (2010): Phase relationships of North Atlantic ice-rafted debris and surface-deep climate proxies during the last glacial period.- Quat. Sci. Rev. 29: 3875-3886, doi: 10.1016/j.quascirev.2010.09.006

Hopkins, T.S. (1991): The GIN Sea-A synthesis of its physical oceanography and literature review 1972-1985.- Earth Sci. Rev. 3-4: 175-318, doi: 10.1016/0012-8252(91)90001-V

Kellogg, T.B. (1980): Paleoclimatology and paleo-oceanography of the Norwegian and Greenland seas: glacial-interglacial contrasts.- Boreas 9: 115-137, doi: 10.1111/j.1502-3885.1980.tb01033.x

Kylander, M.E., Lind, E.M., Wastegård, S. & Löwemark, L. (2012): Recom-

mendations for using XRF core scanning as a tool in tephrochronology.- The Holocene 22: 371-375, doi: 10.1177/0959683611423688

Lacasse, C. (2001): Influence of climate variability on the atmospheric transport of Icelandic tephra in the subpolar North Atlantic.- Glob. Planet. Change 29: 31-55, doi: 10.1016/S0921-8181(01)00099-6

Lacasse, C. & Garbe-Schönberg, C.D. (2001): Explosive silicic volcanism in Iceland and the Jan Mayen area during the last 6 Ma: Sources and timing of major eruprtions.- J. Volcanol. Geotherm. Res. 107: 113-147, doi: 10.1016/S0377-0273(00)00299-7

Lacasse, C., Sigurdsson, H., Carey, S., Paterne, M. & Guichard, F. (1996): North Atlantic deep-sea sedimentation of Late Quaternary tephra from the Iceland hotspot.- Mar. Geol. 129: 207-235, doi: 10.1016/0025-3227(96)83346-9

Latarius, K. & Quadfasel, D. (2016): Water mass transformation in the deep basins of the Nordic Seas: Analyses of heat and freshwater budgets.- Deep. Res. Part I 114: 23-42.

Lessing, P., Decker, R.W. & Reynolds Jr.,R.C. (1963): Potassium and rubidium distribution in Hawaiian lavas.- J. Geophys. Res. 68: 5851-5855.

Lisitzin, A.P. (2002): Sea-Ice and Iceberg Sedimentation in the Ocean: Recent and Past.- Springer Science & Business Media

März, C., Stratmann, A., Matthiessen, J., Meinhardt, A.K., Eckert, S., Schnetger, B., Vogt, C., Stein, R. & Brumsack, H.J. (2011): Manganese-rich brown layers in Arctic Ocean sediments: Composition, formation mechanisms, and diagenetic overprint.- Geochim. Cosmochim. Acta 75: 7668-7687, doi: 10.1016/j.gca.2011.09.046

Ohlendorf, C., Wennrich, V. & Enters, D. (2015): Experiences with XRF-Scanning of Long Sediment Records.- in: Micro-XRF Studies of Sediment Cores, 351-372, doi: 10.1007/978-94-017-9849-5_13

Rasmussen, T.L., Wastegård, S., Kuijpers, A., Van Weering, T.C.E., Heinemeier, J. & Thomsen, E. (2003): Stratigraphy and distribution of tephra layers in marine sediment cores from the Faeroe Islands, North Atlantic.- Mar. Geol. 199: 263-277, doi: 10.1016/S0025-3227(03)00219-6

Risebrobakken, B. (2003): A high-resolution study of Holocene paleoclimatic and paleoceanographic changes in the Nordic Seas.- Paleoceanography 18: 1017.

Risebrobakken, B., Balbon, E., Dokken, T., Jansen, E., Kissel, C., Labeyrie, L., Richter, T. & Senneset, L. (2006): The penultimate deglaciation: High-resolution paleoceanographic evidence from a north-south transect along the eastern Nordic Seas.- Earth Planet. Sci. Lett. 241: 505-516, doi: 10.1016/j.epsl.2005.11.032

Risebrobakken, Dokken, T., Smedsrud, L.H., Andersson, C., Jansen, E., Moros, M. & Ivanova, E.V., (2011): Early Holocene temperature variability in the Nordic Seas: The role of oceanic heat advection versus changes in orbital forcing.- Paleoceanography 26: 1-17, doi: 10.1029/2011PA002117

Schäfer, P., Thiede, J., Gerlach, S., Graf, G., Suess, E. & Zeitzschel, B. (2001): The Environment of the Northern North-Atlantic Ocean: Modern Depositional Processes and their Historical Documentation.- In: P. SCHÄFER, W. RITZRAU, M. SCHLÜTER & J. THIEDE (eds), The Northern North Atlantic: A Changing Environment, Springer, Berlin, 1-17.

Sejrup, H.P., Haflidason, H., Kristensen, D.K. & Johnsen, S.J. (1995): Last interglacial and Holocene climatic development in the Norwegian Sea region: ocean front movements and ice-core data.- J. Quat. Sci. 10: 385-390.

Sjøholm, J., Sejrup, H.P., Furnes, H., Sejrup, H.P. & Furnes, H. (1991): Quaternary volcanic ash zones on the Iceland Plateau, southern Norwegian Sea.- J. Quat. Sci. 6: 159-173, doi: 10.1002/jqs.3390060205

Solignac, S., De Vernal, A. & Hillaire-Marcel, C. (2004): Holocene sea-surface conditions in the North Atlantic – Contrasted trends and regimes in the western and eastern sectors (Labrador Sea vs. Iceland Basin).- Quat. Sci. Rev. 23: 319-334, doi: 10.1016/j.quascirev.2003.06.003

Telesiński, M.M., Spielhagen, R.F. & Bauch, H.A. (2014): Water mass evolution of the Greenland sea since late glacial times.- Clim. Past 10: 123-136, doi: 10.5194/cp-10-123-2014

Thorarinsson, S. (1944): Tefrokronologiska studier pa Island (Tephrochronological studies in Iceland).- Geogr. Ann. 26: 1-217, doi: 10.2307/519916

Tjallingii, R. (2006): Application and quality of X-Ray Fluorescence core scanning in reconstructing late Pleistocene NW African continental margin sedimentation patterns and paleoclimate variations.- Diss. Thesis, Dep. Geosci. Univ. Bremen.

Van Nieuwenhove, N., Bauch, H.A. & Matthiessen, J. (2008): Last interglacial surface water conditions in the eastern Nordic Seas inferred from dinocyst and foraminiferal assemblages.- Mar. Micropaleontol. 66: 247-263, doi: 10.1016/j.marmicro.2007.10.004

Wallrabe-Adams, H.J. & Lackschewitz, K.S. (2003): Chemical composition, distribution, and origin of silicic volcanic ash layers in the Greenland-Iceland-Norwegian Sea: Explosive volcanism from 10 to 300 ka as recorded in deep-sea sediments.- Mar. Geol. 193: 273-293, doi: 10.1016/S0025-3227(02)00661-8

Wastegård, S. & Rasmussen, T.L. (2001): New tephra horizons from Oxygen Isotope Stage 5 in the North Atlantic: Correlation potential for terrestrial, marine and ice-core archives.- Quat. Sci. Rev. 20: 1587-1593, doi: 10.1016/S0277-3791(01)00055-5

Wolf, T.C.W. & Thiede, J. (1991): History of terrigenous sedimentation during the past 10 m.y. in the North Atlantic (ODP Legs 104 and 105 and DSDP Leg 81).- Mar. Geol. 1-4: 82-102, doi: 10.1016/0025-3227(91)90064-B

Zhuravleva, A., Bauch, H.A. & Van Nieuwenhove, N. (2017): Last Interglacial (MIS 5e) hydrographic shifts linked to meltwater discharges from the East Greenland margin.- Quat. Sci. Rev. 164: 95-109, doi: 10.1016/j.quascirev.2017.03.026

Ziegler, M., Jilbert, T., De Lange, G.J., Lourens, L.J. & Reichart, G.J. (2008): Bromine counts from XRF scanning as an estimate of the marine organic carbon content of sediment cores.- Geochemistry, Geophys. Geosystems. 9: 1-6, doi: 10.1029/2007GC001932